High-speed ultra-accurate direct C2W bonding

Birgit Brandstätter, Daniel Aschenwald, Benedikt Auer, Norbert Bilewicz, Ruurd Boomsma, Christoph Kröll, Andreas Mayr, Richard Neumayr, Hannes Rieser, Mario Schernthaner, Hubert Selhofer, Florian Speer, Peter Unterwaditzer, András Vidéki, Martin Widauer, Thomas Widmann

R&D Process Development
Besi Austria GmbH
6241 Radfeld, Austria
e-mail: Birgit.Brandstaetter@besi.com

***Abstract*—Chip-to-wafer hybrid bonding is needed as contact pitch and pad size decrease to the single micrometer range (5 micrometer or lower). Here, classical bonding technologies like themo-compression bonding and flip-chip with mass reflow are no longer sufficient, and hybrid bonding emerges as an attractive alternative. While the technology is well known in wafer-to-wafer processing, for chip-to-wafer at industrial speed and accuracy, new placement technologies and deeper understanding of accuracy behavior during the bonding process both are essential. This paper describes new optical recognition methods for small pads for accurate in-situ alignment before the bonding stroke as well as a new bond-head design and behavior for accurate placement at 200 nm at each point of the die, including large dies, and at speeds of 2000 units per hour.**

Keywords-hybrid bonding, dielectric bonding, chip-to-wafer, flip-chip, fine pitch, optical recognition, high throughput, high accuracy, precision

I. INTRODUCTION

Hybrid bonding is used in advanced packaging for 2.5D and 3D applications when sub 5-micrometer pitches and/or low profile 3D stacks are targeted. The term `hybrid bonding´ stands for the combination of dielectric bonding and direct metal-to-metal (e.g. Cu-to-Cu) bonding [1][2][3][4]. Wafer-to-wafer (W2W) based hybrid bonding is already in mass production for image sensors [1][4] and some other applications. For through 3D silicon via (TSV) stacks and heterogeneous 2.5D integration, however, there is an increasing demand for chip-to-wafer (C2W) based hybrid bonding solutions [1], which for pitches of 1 µm to 5 µm would open the door to an area interconnection density of 40.000 to 1 million bumps per square millimeter and beyond. Such integration has the potential to overcome the performance limitation inherently introduced by the scaling of CMOS devices [5][6].

Currently, thermo-compression bonding is used for fine pitch C2W stacking. The process, however, needs high force and high-temperature ramps where CTE (coefficient of thermal expansion) mismatch causes deformation and stress and thus limits pitch to around 7 µm [7], besides inherently being a slow and thus cost intensive process. Here, hybrid bonding benefits from low force and room temperature processing, with the potential of offering fast processing and stress-free bonding. Hybrid bonding for C2W and chip-to-chip (C2C), nevertheless, comes with severe technological challenges: Unprecedented placement accuracy below 200 nm at each point of the chip, ISO 3 cleanroom class at the processing area to ensure void-free bond interfaces, and finally, high productivity of > 3000 units per hour (UPH).

This paper presents first results of a hybrid C2W bonder prototype, the Datacon 8800 CHAMEO$^{ultra\ plus}$, with final specification targets of 200 nm @ 3 σ, ISO 3 cleanroom environment and 2000 UPH for 300 mm wafer substrates. The bonder is designed to perform a fully automated pick and place with component flip and a direct C2W bond.

To achieve high accuracy, new alignment and optics hardware for fast, robust, and highly accurate alignment are launched. Such alignment capability is reached by a novel set of cameras which determine the component and bond position prior and while aligning the die with unseen accuracy [9]. The mechanical alignment concept further relies on high-precision piezo actuators performing critical final positioning steps.

Void-free bonding is made possible by a clean machine concept as presented together with a clean air flow concept.

Finally, tests with silicon dies and silicon oxide finish and corresponding substrate wafers were evaluated. Accuracy is determined by IR inspection, voids at the bond interface as an indicator of contamination were made visible with acoustic microscopy. Productivity is measured and presented.

II. C2W BONDING AND MACHINE TECHNOLOGY

A. Machine concept

Fig. 1 shows the working area of Besi's direct bond C2W prototype, the Datacon 8800 CHAMEO$^{ultra\ plus}$. The machine comprises the component wafer table (below the working area), the substrate wafer table, and two mirrored pick-and-place systems (including flipper, cameras, and moving bond heads) working simultaneously on one substrate and component wafer for double throughput.

A pick-and-place cycle starts with component recognition on the component wafer with the wafer camera. An individual chip is selected, ejected with the ejector needles, picked up with the flipper (either left or right), flipped, and transferred to the pick & place tool (of the corresponding side). Next, the bond head moves the die over the up-looking (component) camera which determines the exact position of the die on the pick-and-place tool. Hereafter, the bond head moves to the substrate position, and the substrate (downward) camera detects the exact bonding position on the substrate. Sub-micrometer alignment is performed with piezo-actuated drives, and in-situ alignment during accuracy movements is

2377-5726/20/$31.00 ©2020 IEEE
DOI 10.1109/ECTC32862.2020.00303

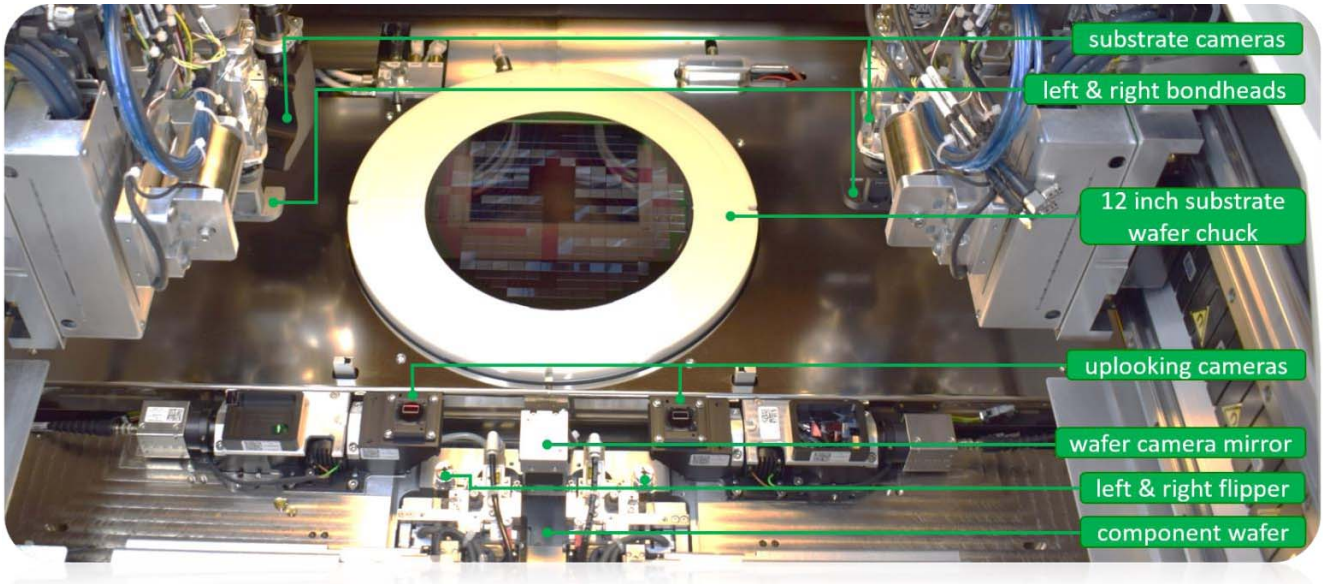

Fig. 1. Working area of the Datacon 8800 CHAMEO$^{ultra\ plus}$. The machine is able to process 300 mm substrate and component wafers in an ISO 3 cleanroom environment. Two bond heads, flippers, and camera systems work in parallel on one substrate and component wafer to double throughput.

used to further optimize the die position. Finally, the bond head places the die onto the bonding position with the selected bond force and bond delay. The cycle is performed in parallel for left and right side and is repeated until a substrate is fully populated.

The machine automatically changes substrate and component wafers as required for the production flow. Thus, material delivery and storage compartments are integrated in the system to automatically load and unload, align and transfer wafers onto the bond stage, often employing FOUPs (front opening unified pods).

B. Alignemnt concept for high accuracy

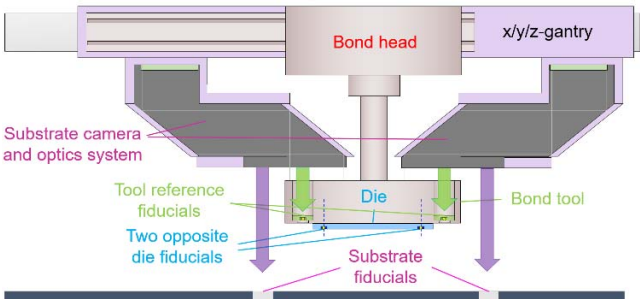

Fig. 2. Schematic of the substrate vision setup. Two separate substrate cameras are capable of seeing substrate and bond tool fiducials at opposing substrate corners simultaneously. The bond head is mounted moveable with respect to the cameras for in-situ fine alignment.

The new Datacon 8800 CHAMEO$^{ultra\ plus}$ achieves extreme alignment accuracy through a novel vision and alignment concept. The core idea is based on glass-based reference marks which are seen with both, the component (up-looking) camera and the substrate (downward) camera. The component to substrate distance metrology greatly benefits of the highly accurate measurement of two marks (component and reference and substrate and reference, respectively) in the same calibrated field of view (FoV). Fig. 2 shows the alignment concept for substrate vision.

The reference-fiducial marks are integrated in the pick-and-place bond tool and are visible from above with the substrate camera system and from below with the upward component camera. After component pick, the up-looking camera references component fiducial and tool reference fiducial with respect to each other. Usually, the component size is larger than the component camera field of view (~4 mm x 4 mm). Thus two images close to two component corners are taken as robust component position and rotation reference. Next, the bond head moves the die to the (approximate) substrate position. There, the substrate camera system references the substrate fiducials to the tool reference fiducials. This substrate camera system is made up of two separate lens systems and camera chips, each of which is set up to see one substrate corner and bond-tool corner with reference fiducials, again, in one field of view. Using these four images with component and substrate information with respect to the tool reference, the machine calculates the exact offset between component fiducials and substrate fiducials. Subsequently, a micro positioning system compensates the calculated offset. Accuracy of those micro movements is verified again with the substrate camera system, thus enabling an in-situ verification of substrate-to-component position. Finally, the bond head moves down to place the component. This final bond stroke movement is kept small (~ 0.5 mm) to avoid additional misalignment.

The optical setup of all cameras is such that small pads and fiducial can be detected with high precision, and that the setup is adaptable to different component sizes up to 30 mm edge length [7]. Customized optical components employ multiple focus levels in a single field of view and enable sharp mapping of tool reference fiducials and material fiducials on different height levels in the same image.

C. *Image processing accuracy*

The placement accuracy critically relies on the capability to detect substrate, component, and tool reference positions with very high accuracy in the camera FoV, and fiducial position uncertainty should be negligible with respect to the target accuracy. Hence, an optimal combination of low sensor noise, high image contrast (good illumination), good fiducial form and fiducial size, and an elaborate FoV calibration are crucial.

Besi employs numerous calibration routines to derive the extrinsic parameters of the camera system and subsequently allow high-accuracy extraction of intrinsic parameters such as fiducial positions.

Regarding fiducial quality, highly accurate search fiducials of good contrast are required to allow for robust pixel averaging. Digital image processing then extracts fiducial shape and position with a specific measurement uncertainty.

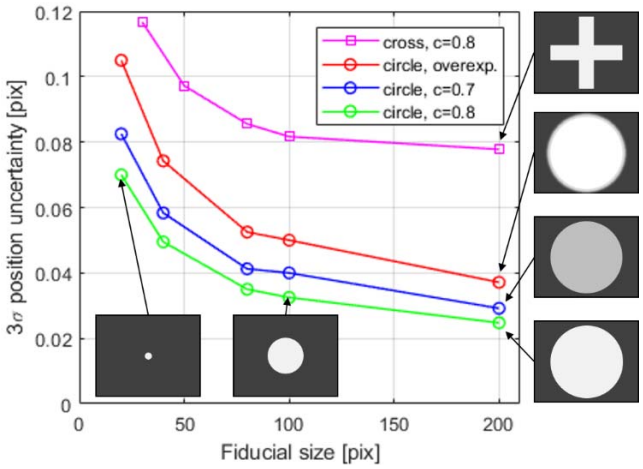

Fig. 3. Position uncertainty of circular and cross shaped fiducials of varying contrast as a function of size. The best accuracy of 1/40th of a pixel is reached with a large circular fiducial of contrast c = 0.8.

Fig. 3 shows measurements of the fiducial position uncertainty as a cross shaped and a circular fiducial are moved in the camera FoV with a nanometer stage. Each fiducial shape is analyzed in five different sizes. The stage position is compared with the vision measurement. For the cross shaped fiducial, systematic errors for finding the position of edges are confirmed in the measurements and become significant in the required accuracy range. As stated further in [10][11][12], fiducials which employ lines become less reliable at such scales. In contrast, a circular fiducial gives best position results. Hence, a more detailed look on circles is taken.

Theoretic rules to estimate position uncertainty, σ_x and σ_y, of the circle midpoint coordinates, x and y, with respect to size and contour noise are found in [13].

$$\sigma_x = \sigma_y = \frac{1.42\ \sigma_p}{\sqrt{N}} \qquad (1)$$

The variable N is the number of extracted circumference points proportional to the diameter or resolution of a circular fiducial. The N contour points p_i of a circle fiducial represent the extracted circumference points by image processing. Hence, σ_p can be interpreted as the sum of errors of sensor noise, contrast, and fitting algorithm, if these cause stochastic, independent Gaussian noise. As such, the parameter σ_p indicates the circle-fitting uncertainty, and the standard deviations of the Gaussian probability density function, σ_x and σ_y, give an estimate of circle fitting position reproducibility.

The Michelson contrast definition is used to quantify the relationship between bright and dark features as

$$c = \frac{I_{max} - I_{min}}{I_{max} + I_{min}} \qquad (2)$$

with I_{max} and I_{min} representing the highest and lowest luminance. Overexposure or insufficient contrast both increase the circle fitting uncertainty σ_p, and thus increase the fiducial position uncertainties on σ_x and σ_y.

For the Datacon 8800 CHAMEO$^{ultra\ plus}$ substrate and component camera optics, the diffraction limit is ~3 µm. Cameras and optics feature 12 Mpix and a resolution of 1.15 µm / pixel. Thus camera resolution exceeds the diffraction limit. However, when looking at large structures (such as search fiducials), diffraction only decreases object sharpness. Above measurements show that search accuracies of 1/40th pixel (corresponding to less than 30 nm @ 3 σ uncertainty) for appropriate fiducials are reached.

D. *Position stability and motion capability*

The machine accuracy furthermore critically relies on position stability and motion control's set-point accuracy.

During component placement, both, component and substrate must be held in place virtually without vibration or other agitation. Thus, any source of machine internal disturbance, such as rotating fans and transformers, must either be mounted with insulation or eliminated. Similarly, for the machine grounding, it is essential to damp out vibrations and not to introduce further noise into the system from outside.

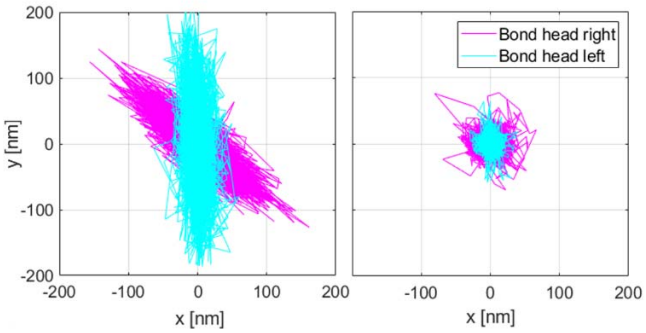

Fig. 4. Bond-head stability as a function of machine grounding. Left: vibration noise >150 nm @ 3 σ is coupled into the machine from outside. Right: <50 nm @ 3 σ with good grounding.

Fig. 4 shows stability measurements of left and right bond heads as the machine is positioned on two different groundings. For the measurement, the substrate cameras record the center position of a fiducial on the substrate. Offsets of x and y indicate vibrations between substrate and bond

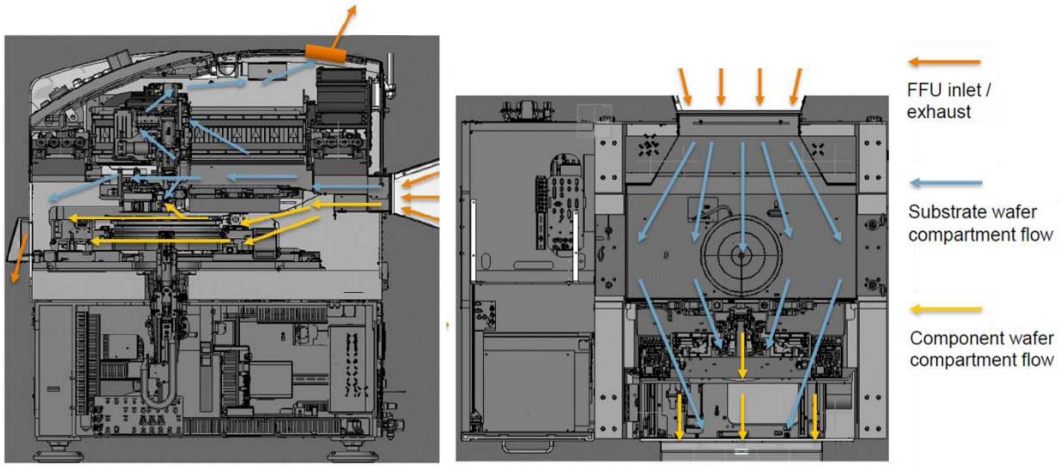

Fig. 5. Machine side view (left) and top view (right) with indicated clean air-flow concept through substrate-wafer and component-wafer compartments. The fan-filter unit (FFU) provides filtered air which is steered in linear flow above critical surfaces.

head. Fig. 4 left shows data with the machine placed on the same floor as another moving pick-and-place machine. Here, vibration noise exceeds 150 nm @ 3 σ on both bond heads. Fig. 4 right shows data of the machine mounted on a low-vibration ground. Here, both bond heads are stable below 50 nm @ 3 σ.

Additionally, movable axes need to be of extremely low vibrational noise when at rest such that active position encoders hold a set position virtually without vibration.

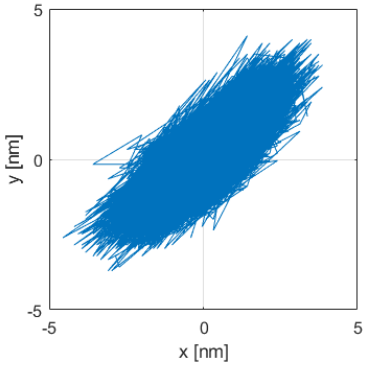

Fig. 6. Vibration noise of the θ- and z-axis air bearing while holding a set point.

Finally, high quality bearings need to be used. Beside many advantages such as minimum friction (which avoids hysteresis) and minimal linear and radial run-out, air bearings have the disadvantage of self-excited vibration. A vibration measurement is performed of the Datacon 8800 CHAMEO$^{ultra\ plus}$ angular (θ-) and z-axis air bearing. A laser interferometer records movements of x- and y-positions (at set point) of the bond tool at a sampling frequency of 10 kHz and with a measurement accuracy better than 4 nm @ 3 σ. Fig. 6 shows this vibration noise of the air bearing to be 5 nm @ 3 σ (3 σ_x = 3.6, 3 σ_y = 3.4 nm). The result is dominated by measurement noise, verifying that, the bearing in use is well designed to keep vibration noise below critical values.

Next to mechanical stability, each axis (x, y, and θ) needs at least one positioning system with nanometer accuracy for final alignment. To achieve such accuracy in x and y, piezo driven actuators are used with a resolution below 1 nm. Similarly, when moving to large components, angular alignment capability becomes increasingly critical. The newly designed θ-system for the Datacon 8800 CHAMEO$^{ultra\ plus}$ has a high-accuracy dual-encoder read-head setup for good resolution and to compensate for inherent eccentricity errors.

E. Cleanliness

Silicon-silicon direct-bonding cleanliness requirements are ISO 3 and better in both, the substrate-wafer compartment, where dies are placed on the substrates by the bond heads, and in the component-wafer compartment, where dies are picked. Furthermore, material delivery and storage compartments must fulfill such cleanliness, e.g. FOUP for storage, and the transport system, where the wafers are loaded and unloaded, aligned and transferred onto the bond stage.

Even as ISO 3 airborne particles are reached, for direct bonding, it is more significant to count deposited particles on a wafer passing through the machine. Typical requirements for `particles per wafer pass´ are that no particles > 0.5 µm and less than 10 particles between 0.2 µm to 0.5 µm are found after processing.

To reach such high cleanliness in the Datacon 8800 CHAMEO$^{ultra\ plus}$, a fan-filter unit (FFU) provides filtered air into substrate- and component-wafer compartments for air refreshment and to provide a protective air curtain above the critical surfaces. Fig. 5 shows the air flow through the machine, where clean air enters at the back and is exhausted at the front.

Additionally, cleanliness is optimized through appropriate component materials, design and sourcing as well as clean machine assembly.

F. Process capability

The C2W hybrid bonding process requires a series of advanced material processing steps: CMP (chemical mechanical polishing) of both, substrate and component wafers, component wafer dicing and cleaning, plasma activation, and finally, C2W bonding.

The C2W bond must guarantee contamination free component ejection, handling, and flipping, as well as void free bonding. During component ejection and flip, the activated component side is handled with the flip tool which thus is designed to not contaminate or spoil the component surface.

Additionally, the pick-and-place tooling for the C2W bond needs to allow for component – substrate contact being initiated at the die center to avoid formation of voids though entrapped air. Thus, tooling which forces components from their natural shape to a slightly convex curvature is employed. Now, when bringing component and substrate in contact, the bond process starts at the component center, and the bond wave propagates from the center to the edges.

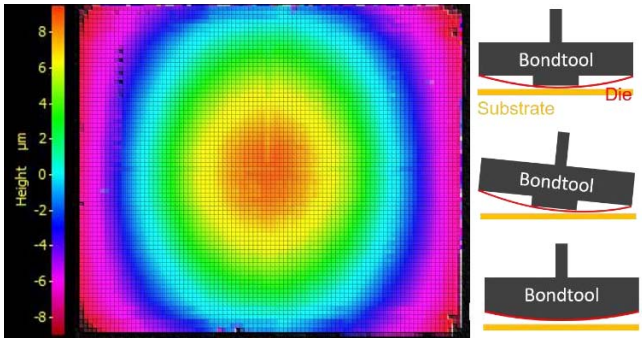

Fig. 7. Left: height measurement showing the convex component shape of a silicon die imposed by special tooling design. Right: Sketches of tools with pedestal and convex surface. Slight component-surface non-parallelism is compensated with convex tools.

Fig. 7 shows a height measurement of a silicon component, visualizing the slight curvature imposed by the tooling shape. Several bond-tool designs are capable of providing such a convex component shape, as illustrated on the left of Fig. 7. Additionally, a convex die shape avoids starting the bond at the component corner in case of slight non-parallelism of die vs. substrate.

III. Experimental Results and Discussion

A. Alignemnt capability

Alignment accuracy is tested with glass material. A substrate (> 300 mm x 300 mm) containing a matrix of circular fiducials is placed in the machine, and a glass die is aligned with respect to multiple substrate positions. Substrate and die have concentric ring fiducials with the same matrix pattern. The large glass die has a component corners fiducial distance of 28.4 mm x 28.4 mm. Over the substrate fiducial matrix, the glass die is aligned with the alignment scheme described in II.A, and post alignment accuracy is measured. After each alignment position, the bond head continues to move on to the next bond position. One measurement run consists of 35 (7 x 5) alignment positions. In these alignment tests, the alignment accuracy is measured without having released the glass die using the substrate camera system.

Fig. 8 shows the alignment results of 16 consecutive measurement runs. Alignment accuracy was measured to be 189 nm @ 3 σ (3 σ_x = 121 nm, 3 σ_y = 118 nm, 3 σ_θ = 298 µ°). Thus, the target specification of 3 σ = 200 nm is reached for large component alignment.

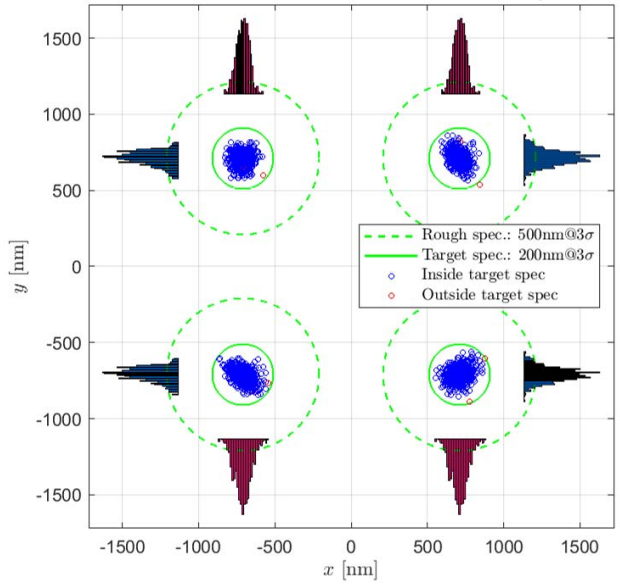

Fig. 8. Alignment accuracy over 35 bond positions and 16 measurement runs. Alignment accuracy measurements of all bond positions overlapped are shown for the 4 component corners. An alignment accuracy of 3σ = 189 nm is measured.

B. Infrared microscopy measurement capability

Bonded test material is analyzed at infrared (IR) wavelength above 1200 nm. Such wavelength allow looking through the silicon chip and making component and substrate fiducials visible for post-bond accuracy measurements. Besi uses an automatic IR microscope (Promicron) for IR image acquisition and processes images with an in-house vision toolbox to perform ultra-accurate position measurements.

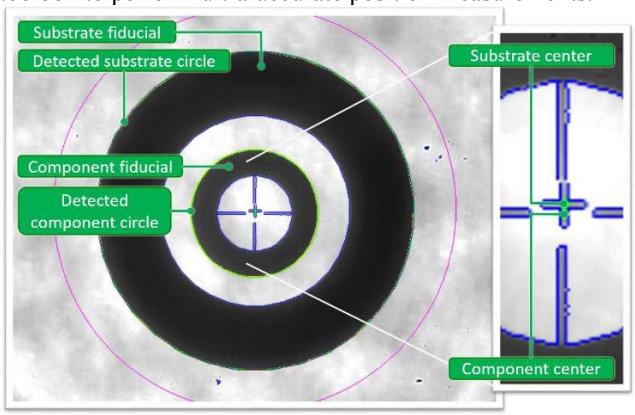

Fig. 9. IR image of a bonded die on substrate. The pixels used by the image processing software for substrate-circle and component-circle center detection are marked in green.

Fig. 9 shows an IR microscope image of a bonded component picturing component fiducial and substrate fiducial acquired through the thin (~200 µm) silicon chip.

Image processing software is set to detect outer substrate-fiducial circle and outer component-fiducial circle and calculates their circle center offsets.

Measurement capability again is critical for the accuracy regime in which test material is analyzed. Thus, the uncertainty with which the center of a circle fiducial is determined is evaluated for the IR microscope.

The following procedure is used: Automated acquisitions of >1000 images of one fiducial ring with outside and inside diameter of 190 µm and 200 µm, respectively, are recorded. The fiducial is moved slightly in x- and y-direction before each image is taken. Image processing then searches the two circular fiducials and determines the circle centers with sub-pixel accuracy for each image. Ideally, the centers of the two circles are identical in each image. The offset of these centers is recorded for each image. The variation of these center offsets represent the measurement repeatability.

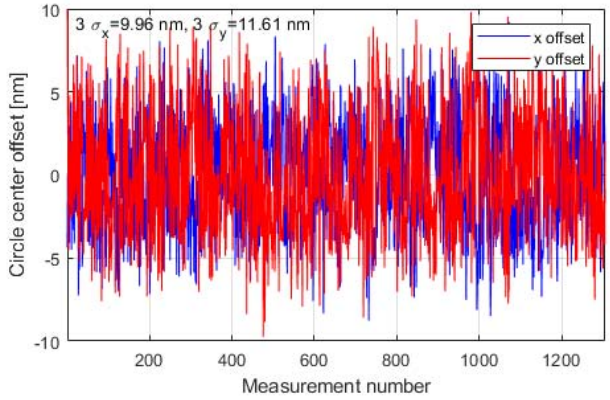

Fig. 10. Center-to-center offset measurement for concentric circular fiducials. The offset is split in x- and y-direction.

Fig. 10 shows results using a microscope objective with 50-fold resolution (0.44 µm/pixel). Silicon chips in this test had a 150 µm thickness. A 3 σ_x = 9.96 nm and 3 σ_y = 11.6 nm measurement uncertainty is achieved.

C. *Direct bonding accuracy and throughput*

The Datacon 8800 CHAMEO$^{ultra\ plus}$ prototype is used for high-speed and high-accuracy C2W direct bonds. Test material of high cleanliness and proper surface preparation is provided by Xperi (Xperi Corperation, CA, USA).

Test chips (11 mm x 8 mm) are ejected from the component wafer, flipped by 180° and transferred to a bond tool. As described, the exact position of the die on the bond tool is determined with the up-looking camera before the chip is brought to the substrate wafer. The exact placement position is determined using the substrate camera system, and iterative positioning steps are performed to reach extreme accuracy for placement before final z-down movement, component and substrate contact and subsequent bond.

After processing, the substrate wafer with the placed components is extracted from the machine. Placement accuracy is measured with the automated IR microscope, qualified in Sec. B. Infrared images of all bond positions are acquired automatically at the bonding interface for four corner and one center fiducial per die, and placement data is extracted using Besi's image processing and analysis software.

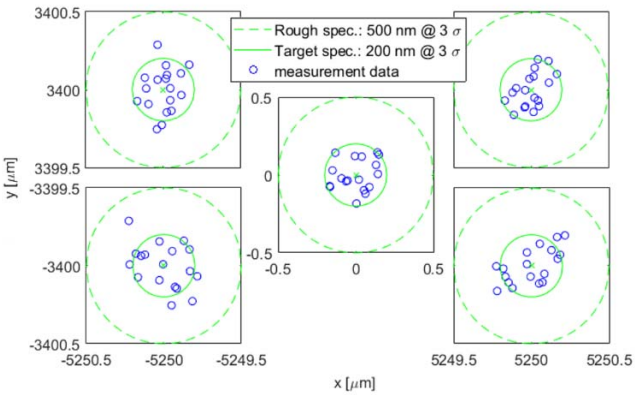

Fig. 11. Post-bond accuracy on the four component corner and the component center fiducials.

Fiducial positions on substrate and component do not correspond exactly to the coordinates of the material drawing. Usually, lithography, production and thermal changes add uncertainties to these ideal positions. In this test, 5 fiducials are used and thus placement accuracy is over-determined. Hence, material accuracy (including the measurement uncertainty) can be calculated. We see that when assuming perfect placement at the component center, corner component fiducials deviate from corner substrate fiducials by 230 nm @ 3 σ.

Subtracting material and measurement uncertainty from the placement results, Fig. 11 shows calculated substrate to component offsets for the four corner and the one center fiducial. Placement accuracy is 3 σ_x = 330 nm, 3 σ_y = 300 nm, 3 σ_θ = 864 µ°.

The timing of all process steps is measured automatically by the pick-and-place machine. While left and right bond heads process the current component, ejection of the next components (for left and right bond head) are executed in parallel such that the flippers present ejected and rotated components to the bond heads once the bonds are finished. The up-looking camera component search is accomplished in 600 ms. The iterative nanometer adjustment of the component to the substrate takes around 1700 ms. Bond head movements to process the component and finally bond delay account for another 1200 ms, bringing the cycle time to process two dies (one on the left and one on the right bond head) to 3.5 s. Thus, a UPH of 2060 is reached.

D. Cleanliness

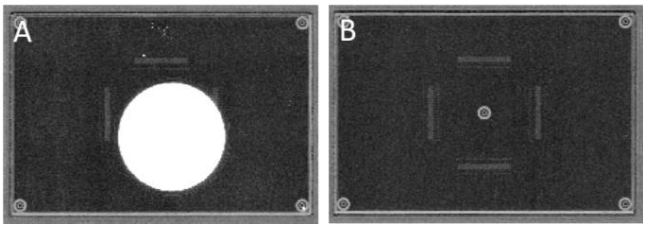

Fig. 12. Scanning acoustic microscope images of bonded chips. A, a large circular void is visible due to a contaminating particle. B, bond between two clean surfaces.

After a batch annealing step, cleanliness and bond quality are assessed through scanning acoustic microscopy.

Fig. 12 shows two acoustic microscope images of bonded chips. The left image shows a circular void due to contamination. The right image represents a fully bonded component using a clean machine and proper setup. The acoustic microscope images were taken at Xperi.

IV. Conclusion and Outlook

A novel equipment is presented capable of high-precision and high-fidelity C2W direct bonding with high throughput. Components of sizes between 6 mm edge length up to 30 mm have been bonded. The high-accuracy alignment capability is verified for such die sizes, and measurement data shows an alignment capability of < 200 nm @ 3 σ for C2W alignment. Particle measurements show < ISO 3 airborne particles, and process tests verify good bonding interface without contamination. IR microscopy measurements show post bond alignment accuracies of ~300 nm @ 3 σ for C2W bonds, and a throughput >2000 UPH. Current bond accuracy is limited by both, alignment accuracy and material fabrication accuracy.

Further developments are planned to increase machine automation and develop a series machine from the first production prototype. For future production needs the machine will be advanced to continuously cater for faster production (higher UPH) and higher accuracy. Here, moving to IR substrate-camera capability will eliminate the need for the up-looking search and enable real in-line C2W position alignment boosting both UPH and accuracy. Active machine mounts to compensate external vibration and counter-act internal machine excitation will allow faster movement with high system stability and thus good accuracy.

All results present the Datacon 8800 CHAMEO$^{ultra\ plus}$ as the C2W direct bond equipment most suitable for realizing next generation high-density devices with 3D technology.

Acknowledgment

Besi acknowledges support by the European Commission and the FFG under the ECSEL program APPLAUSE.

The authors thank Xperi for material production and preparation as well as for scanning acoustic microscope measurements for bond quality analysis.

References

[1] G. Gao, G. Fountain, C. Uzoh, B. Lee, L. Mirkarimi, and L. Wand, "Development of hybrid bond interconnect technology for die-to-wafer and die-to-die applications," International Wafer Level Packaging Conference (IWLPC) 2017.

[2] S. Iyer, "3DSOCs through advanced packaging," 3D ASIP Conference, 2016.

[3] J. Michailos, "Future landscape for 3D integration: from interposers to 3D high density," 3D ASIP Conf., 2016.

[4] T. Nomoto, "Image sensor technology evolution for sensing era," 3D ASIP Conf., 2016, pp. 16-23.

[5] E. Beyne, IEEE Design & Test, 33(3), 8, 2016.

[6] F. Inoue et al. "Influence of Composition of SiCN as Interfacial Layer on Plasma Activated Direct Bonding," ECS Journal of Solid State Science and Technology, 8 (6) P346-P350, 2019.

[7] E. Beyne, "High performance 3D system partitioning and backside power delivery: progress in EDA and 3D integration technology," SMI 3D & Systems Summit, 2020.

[8] "Verfahren für die Montage eines Flipchips auf einem Substrat (Method for the Assembly of a Flip Chip onto a Substrate," European patent EP 1 802 192 A1, 2006.

[9] N. Bilewicz, A. Mayr, H. Pristauz, H. Selhofer, "Apparatus and Method for Mounting Components on a Substrate," US patent, US 2018/0317353, 2018.

[10] L. O'Gorman, A. M. Bruckstein, C. B. Bose, I. Amir, "A comparison of fiducial shapes for machine vision registration," MVA'90, IAPR Workshop on Machine Vision Applications, 1990, pp. 253-256.

[11] M. Hagaraand, P. Kulla, "Edge detection with sub-pixel accuracy based on approximation of edge with erf function," Radio Engineering, 20(2), pp. 516–524, 2011.

[12] E. P. Lyvers, O. R. Mitchell, M. L. Akey, and A. P. Reeves, "Subpixel measurements using a moment-based edge operator," IEEE Trans. Pattern Anal. Mach. Intell., 1989.

[13] P. Schalk, "Metric vision methods for material and product inspection," PhD Thesis, University of Leoben, Austria, 2004